Title: A Physical Expression of Electrons in Density Functional Theory

Authors: Stefano Racioppi[1], Phalgun Lolur[1], Per Hyldgaard[1,2], Martin Rahm[1]*

Affiliations: [1]Department of Chemistry and Chemical Engineering, [2]Department of Microtechnology and Nanoscience—MC2, Chalmers University of Technology; Kemigården 4, Gothenburg, 41258, Sweden.

***Corresponding Author. Email: martin.rahm@chalmers.se**

Abstract: We present a formally exact density functional theory (DFT) determination of the average electron energy. Our orbital-free theory, which is based on a different accounting of energy functional terms, partially solves one well known downside of Kohn-Sham (KS) DFT: that orbital energies have but tenuous connections to physical quantities. Our computed average electron energies are close to experimental ionization potentials in one-electron systems, demonstrating a surprisingly small effect of self-interaction and other exchange-correlation errors in established DFT methods. We argue for the use of the average electron energy as a physics condition on otherwise fictitious KS energy levels and as a design criterion for density functional approximations.

One-Sentence Summary: A formally exact evaluation of average electron energies yields insight into electron dynamics and density functional theory

Main Text: Introduction

Two main factors prevent modern Kohn-Sham (KS) density functional theory (DFT) from producing eigenstates comparable with experimental data: the KS formulation itself and *self-interaction error*. The former is by design used to describe the total electron density as a sum of densities of fictitiously non-interacting electrons. The latter arises as a consequence of describing the total energy as a functional of the electron density,(*1*) and corresponds to the unphysical interactions of electrons with themselves. The self-interaction error is related to more general delocalization and static correlation errors,(*2*) which, together with incorrect asymptotic behaviors of exchange-correlation (XC) potentials,(*3*) are important limitations of DFT. In this work, we present an, in principle, exact DFT determination of the average electron energy, $\bar{\chi}$. This development leads us to derive an on-the-fly correction to KS energy levels that permit a more physical interpretation. We also point to the use of $\bar{\chi}$ as a design criteria and quality indicator for density functional approximations.

The average electron energy $\bar{\chi}$ is an inherent property of any system of electrons, for example molecules. The most general definition of $\bar{\chi}$ includes a sum of all one-electron energies with two times that of multi-electron energies,

$$\bar{\chi} = -\frac{1}{N}(E_{1e} + 2E_{ee}) \,, \qquad (1)$$

where *N* is the total number of electrons. The quantity $\bar{\chi}$ reflects a set of energies that define the dynamics of each electron in the presence of interactions with nuclei (E_{1e}) and with the remaining electrons (E_{ee}). Because of the per-electron focus – that $\bar{\chi}$ involves an average over the total number *N* of electrons – the impact of the electron-electron interaction, enters twice in the formal definition.

The use of $\bar{\chi}$ in chemistry and physics is broad. Approximations to $\bar{\chi}$ based on orbital energy averaging(*4*) have, *e.g.*, been productively used to predict properties like Hammett constants, electrophilic reactive sites, and pK_a.(*5*) The same concept also appears in the theoretical framework of moments of the electron distribution.(*6*) Our interest in $\bar{\chi}$ is rooted in its association with electronegativity,(*7–11*) and to its relation with changes in the total energy as,

$$\Delta E = -N\Delta\bar{\chi} - \Delta E_{ee} + \Delta V_{NN} \quad (2)$$

where V_{NN} is the nuclear repulsion energy.(*8*, *9*) Equation (2) highlights the role of average electron energies in governing chemical and physical processes. Some of us have quantified the role of $\Delta\bar{\chi}$ in chemical bond formation using approximate methods,(*8*, *9*) and used it to study the effect of compression on the electronegativity of atoms.(*12*) In one such approach, $\bar{\chi}$ is *estimated* from experiment, as an average of photoionization energies,

$$\bar{\chi}_{IP} = \sum_{i}^{n} \frac{n_i \varepsilon_{i,IP}}{N} \quad (3)$$

where $\varepsilon_{i,IP}$ and n_i are, respectively, the ionization potential and the occupation number associated to the i^{th} molecular or atomic energy level. The ability to estimate $\Delta\bar{\chi}$ experimentally, along with ΔV_{NN} from molecular structures and ΔE from thermochemical data, has merited us to label Eq. (2) as an *experimental quantum chemistry* energy partitioning.(*9*)

Use of methods such as multi-reference configuration interaction (MRCI) offers an exact, if expensive, evaluation of the average electron energy,

$$\bar{\chi} = -\frac{1}{N}\int\left(\tau_L(\boldsymbol{r}) + \upsilon(\boldsymbol{r})\rho(\boldsymbol{r}) + 2\int\frac{P(\boldsymbol{r},\boldsymbol{r}')}{|\boldsymbol{r}-\boldsymbol{r}'|}d\boldsymbol{r}_2\right)d\boldsymbol{r}, \quad (4)$$

where $\tau_L(\boldsymbol{r})$ is the Laplacian form of the kinetic energy density, $\rho(\boldsymbol{r})$ is the electron density, $v(\boldsymbol{r})$ is the nuclear potential, and $P(\boldsymbol{r},\boldsymbol{r}')$ is the diagonal of the two-electron reduced density matrix.(*8*) In practice, such calculations are often prohibitively costly.

The most straightforward computational approximation to Eq. (1) for molecules is an average over occupied electronic levels, the electronic eigenvalues of a 1-determinant wavefunction,

$$\bar{\chi}_{orb} = -\sum_{i}^{n} \frac{n_i \varepsilon_i}{N}, \tag{5}$$

where ε_i and n_i instead denote the eigenvalue and the occupation number associated to the i^{th} orbital.

Equation (5) is the best possible description of $\bar{\chi}$ within HF theory, for which Koopmans theorem rigorously connects each orbital eigenvalue with a vertical ionization potential.(*13*) A physical interpretation of KS orbital energies is famously lost in DFT.(*14*) KS orbitals are often accurate in reflecting the spatial structure of (and hence matrix elements for) actual excitations and charge transfer.(*15*) However, the problem with Eq. (5) is fundamental, for it is only the highest occupied molecular orbital (HOMO) energy that finds a possible physical interpretation in the Janak's theorem,(*16*) as a sudden photoionization excitation energy. Also, it does so only in the thermodynamical limit. For molecules, there are corrections and the theorem relevance is, nowadays, still under debate.(*17*)

Computing the Average Electron Energy, $\bar{\chi}$, in DFT

Our approach for calculating an in principle exact and physically motivated $\bar{\chi}$ boils down to a sum of energy terms that does not involve KS orbitals. We look first at the components of the exact Eq. (4) so to identify the analogous expressions in KS DFT. The first integral in Eq. (4), $\int \tau_L(\boldsymbol{r})d\boldsymbol{r}$, corresponds to the expectation value of the total kinetic energy $< T >$. In KS DFT, the total kinetic energy is described as a sum of two terms,

$$\int \tau_L(\boldsymbol{r})d\boldsymbol{r} =< T >= T_{KS}[\rho] + T_c[\rho], \quad (6)$$

where $T_{KS}[\rho]$ is the kinetic energy computed by considering a single Slater determinant of the KS orbitals and where the remainder $T_c[\rho]$ is the kinetic correlation energy. In other words, $T_c[\rho]$ is the difference in kinetic energy between the non-interacting (fictitious KS orbitals) and the real interacting electrons we aim to describe. The division of Eq. (6) reflects the breakthrough provided by the KS scheme,(*18–20*) but is also a consequence of there being no direct way to exactly compute the actual kinetic energy < T > in DFT. The correlation component of the kinetic energy is typically handled implicitly, as part of the total XC energy E_{xc}.(*18, 19*) Undoing the division expressed as Eq. (6) is key to our proposed DFT calculation of average electron energies.

The second integral in Eq. (4) describes the energy of the electrons in the field generated by the nuclear charges. Because DFT provides us with access to the ground-state electron-density solution, this nuclear-electron attraction $E_{Ne}[\rho]$ energy can be evaluated exactly,

$$\int v(\boldsymbol{r})\rho(\boldsymbol{r})d\boldsymbol{r} = E_{Ne}[\rho]. \quad (7)$$

The last term of Eq. (4), given by the double integral $\iint \frac{P(\boldsymbol{r},\boldsymbol{r}_2)}{|\boldsymbol{r}-\boldsymbol{r}_2|} d\boldsymbol{r}d\boldsymbol{r}_2$, equals the expectation value of the E_{ee} energy and is in DFT terminology expressed as a sum of terms,

$$\iint \frac{P(\boldsymbol{r},\boldsymbol{r}_2)}{|\boldsymbol{r}-\boldsymbol{r}_2|} d\boldsymbol{r}d\boldsymbol{r}_2 =< V_{ee} >= J[\rho] + E_{xc}[\rho] - T_c[\rho], \quad (8)$$

where $J[\rho]$ denotes the Hartree or mean-field approximation to < E >. This formulation follows from the definition of the XC energy, $E_{xc}[\rho] =< T + V_{ee} > -J[\rho] - T_{KS}$,(*19, 21*) since $T_c[\rho]$ is just the difference between the actual kinetic energy and T_{KS}, the kinetic energy of a single Slater determinant of KS orbitals.(*19*)

By combining Eq. (4) with Eqs. (7-8), we arrive at the formally exact DFT-based determination of the averaged electron energy:

$$\bar{\chi}_{DFT} = -\frac{1}{N}\big(T[\rho] + E_{Ne}[\rho] + 2\cdot(J[\rho] + E_{xc}[\rho] - T_c[\rho])\big). \quad (9)$$

Equation (9) is *mostly* given in terms provided by generic orbital-based and planewave DFT codes. We do, however, need a separate step for computing the $T_c[\rho]$ term, which we outline in the SI. Fortunately, the $T_c[\rho]$ term is often small compared to the total XC energy in molecules, where exchange dominates. In cases where this assumption holds in practice we may proceed with an approximate characterization,

$$\bar{\chi}_{DFT} \approx \bar{\chi}_{DFT*} = -\frac{1}{N}\big(T_{KS}[\rho] + E_{Ne}[\rho] + 2\cdot(J[\rho] + E_{xc}[\rho])\big), \quad (10)$$

where all terms are directly available in orbital based DFT codes. We shall use this approximation for the analysis below because we have documented that, for the set of investigated molecules, the ratio of T_c and E_{xc} is at most 6 percent (Table S1).

The $\bar{\chi}_{DFT}$ and $\bar{\chi}_{DFT*}$ quantities are both notably different from HF *and* KS orbital-based approximations, $\bar{\chi}_{orb}^{HF}$ and $\bar{\chi}_{orb}^{KS}$, commonly computed in chemistry from Eq. (5).(*4–6*, *11*, *12*, *22*) Equation (5) and the exact Eq. (4) are identical at the HF level. However, an averaging over KS orbital energies also reflects a density-weighted integral of the XC potential, $v_{xc}(\boldsymbol{r})$ (*18*),

$$\bar{\chi}_{orb}^{KS} = -\sum_{i}^{n}\frac{n_i\varepsilon_i}{N} = -\frac{1}{N}\left(T_{KS}[\rho] + E_{Ne}[\rho] + 2J[\rho] + \int v_{xc}(\boldsymbol{r})\rho(\boldsymbol{r})d\boldsymbol{r}\right). \quad (11)$$

In short, we now have: $\bar{\chi}_{DFT} \approx \bar{\chi}_{DFT*} \neq \bar{\chi}_{orb}^{KS}$, three robust methods through which the average electron energy $\bar{\chi}$ can be calculated using DFT. They all deliver at varying degrees of approximation for even the formally exact expression relies on non-exact XC energy functionals.

In what follows, we focus on the analysis of $\bar{\chi}_{DFT*}$ and comparisons with estimates of $\bar{\chi}$ from HF and KS-orbitals ($\bar{\chi}_{orb}^{HF}$ and $\bar{\chi}_{orb}^{KS}$ *viz*. Eq. (5)), MRCI calculations ($\bar{\chi}^{MRCI}$ *viz*. Eq. (4)), and with experimental photoionization data ($\bar{\chi}_{IP}$ *viz*. Eq. (3)). To facilitate for a thorough comparison between $\bar{\chi}_{DFT*}$ and $\bar{\chi}_{orb}^{KS}$, we rely on two popular XC functionals, PBE (*23*) (providing $\bar{\chi}_{DFT*}^{PBE}$ and $\bar{\chi}_{orb}^{PBE}$) and B3LYP (*24*, *25*) (providing $\bar{\chi}_{DFT*}^{B3LYP}$ and $\bar{\chi}_{orb}^{B3LYP}$). We will at times refer to our $\bar{\chi}_{DFT*}$-values as *XC corrected* average electron energies.

Results

***One-electron Systems*.**

The self-interaction error of DFT is most apparent in systems of only one electron. The XC energy functional must here produce an effective local XC potential that exactly cancels what is clearly a spurious Hartree or mean-electron-field energy contribution to $J[\rho]$.(*1*) For one-electron systems $\bar{\chi}$ *should* equal the total energy of the system.

Table 1 shows $\bar{\chi}$ calculated in different ways for three one-electron systems: H, He^+ and H_2^+. Also shown are experimental references, $\bar{\chi}_{IP}$, which in these cases are nothing more than the single ionization potential of the molecule or ion in question. Note in Table 1 the clearly unphysical energies of the KS-orbitals ($\bar{\chi}_{orb}^{PBE}$ and $\bar{\chi}_{orb}^{B3LYP}$ are here the negative of the energies of occupied KS energy levels). For example, the KS-orbital of H is attributed an energy of 7.6 and 8.8 eV with PBE and B3LYP, respectively. The actual energy of an electron in H is exactly the ionization potential of the atom, 13.598 eV.

Table 1: Average electron energies $\bar{\chi}$ of one-electron systems in $eV \cdot e^{-1}$, estimated at varying levels of approximation.

	$\bar{\chi}_{orb}^{PBE}$	$\bar{\chi}_{orb}^{B3LYP}$	$\bar{\chi}_{DFT*}^{PBE}$	$\bar{\chi}_{DFT*}^{B3LYP}$	$\bar{\chi}_{orb}^{HF}$	$\bar{\chi}^{MRCI}$	$\bar{\chi}_{IP}{}^{a}$
H	7.574	8.767	13.614	13.745	13.604	13.605	13.598
He^+	42.038	44.510	54.098	54.356	54.418	54.419	54.418
H_2^+	23.772	25.004	30.414	30.450	30.017	30.019	30.005

[a] Computed from Eq. (3) and experimental data detailed in the supplementary text.

The improvement provided by Eq. (10) is drastic: $\bar{\chi}_{DFT*}$ is already with a conventional generalized-gradient-approximation (GGA) functional, such as PBE, in near perfect agreement with experiment. The value of $\bar{\chi}_{DFT*}^{PBE}$ for H is, likely somewhat fortuitously, only 16 meV different from experiment. The hybrid XC functional B3LYP is less affected by self-interaction error overall, but overestimates the electron energy in H by 0.14 eV.

Two-electron Systems.

In Table 2, we next compare two-electron systems: He, H_2 and H^-. With a second electron correlation energy is introduced, and we here expect the mean-field picture of HF to fail to some degree. In principle, the energy of two explicitly correlated electrons should be better described by DFT.

Table 2: Average electron energies $\bar{\chi}$ of two-electron systems in $eV \cdot e^{-1}$, estimated at varying levels of approximation.

	$\bar{\chi}_{orb}^{PBE}$	$\bar{\chi}_{orb}^{B3LYP}$	$\bar{\chi}_{DFT*}^{PBE}$	$\bar{\chi}_{DFT*}^{B3LYP}$	$\bar{\chi}_{orb}^{HF}$	$\bar{\chi}^{MRCI}$	$\bar{\chi}_{IP}$
H^-	-3.328	-2.432	1.294	1.563	0.398	1.571	0.800
He	15.734	17.986	25.998	26.552	24.976	26.601	24.587
H_2	10.378	11.827	17.109	17.478	16.176	17.689	15.980

Indeed, whereas the estimates based on averaging KS orbital energies, are far off the mark and predict unbound electrons, the corrected $\bar{\chi}_{DFT*}^{PBE}$and $\bar{\chi}_{DFT*}^{B3LYP}$-values are all slightly larger than the negative of the HF orbital energies, $\bar{\chi}_{orb}^{HF}$. In other words, our $\bar{\chi}_{DFT*}$ evaluations correctly describe electrons that are *more bound* compared to the mean field description. Adding the T_c contributions to extract $\bar{\chi}_{DFT}$ increases the values only marginally (table S1). The improvements provided by the near exact $\bar{\chi}_{DFT*}$ is further highlighted when comparing to MRCI results. MRCI introduces, at considerable computational costs, correlation energy contributions which are missed in HF theory. Going forward, $\bar{\chi}^{MRCI}$ (and *not* $\bar{\chi}_{IP}$) represents our reference values for validating Eq. (10) in multielectron systems. Whereas photoionization experiments can provide highly accurate measurements of the electron energy in one-electron systems (Table 1), the comparison becomes approximate for multielectron systems.

The reason why $\bar{\chi}_{IP}$ is only approximately equal to $\bar{\chi}$ for systems of more than one electron is that ionization is a process between two states. In contrast, $\bar{\chi}$ is, per definition in Eq. (1), a property of one state. Relaxation of the electronic structure, *e.g.*, spatial contraction of orbitals, upon ionization is the reason why we should expect measures of $\bar{\chi}_{IP}$ to systematically underestimate the actual average electron energy $\bar{\chi}$.(*26, 27*) Indeed, in Table 2, and in all data thereafter, our $\bar{\chi}_{DFT*}$ and $\bar{\chi}^{MRCI}$ estimates to $\bar{\chi}$ are consistently larger, *i.e.*,

show *more strongly bound electrons*, compared to estimates from experimental photoionization, $\bar{\chi}_{IP}$. Ionization of single molecules can, of course, be calculated very accurately, especially with MRCI. However, averaging of such accurate ionization energies, *cf.* Eq. (4) does not exactly equal $\bar{\chi}$.

Larger Molecules.

Table 3 shows comparisons of approximations to $\bar{\chi}$ in larger molecules. The real take-away from Table 3 is the notable agreement in absolute values of, $\bar{\chi}_{DFT*}^{PBE}$, $\bar{\chi}_{DFT*}^{B3LYP}$ and $\bar{\chi}^{MRCI}$. Our XC-corrected average electron energies $\bar{\chi}_{DFT*}$ are also systematically larger than $\bar{\chi}_{orb}^{HF}$. We can attribute the difference in energy to the missing correlation energy in a HF description. For example, by removing the $E_c[\rho]$ contribution (tables S2-3) from our $\bar{\chi}_{DFT*}^{PBE}$ and $\bar{\chi}_{DFT*}^{B3LYP}$ estimates for CO_2, the latter compute as 147.52 eV·e^{-1} and 147.33 eV·e^{-1}, respectively, comparable to the 147.99 eV·e^{-1} for $\bar{\chi}_{orb}^{HF}$.

Table 3: Average electron energies $\bar{\chi}$ of a selection of molecules in eV·e^{-1}, estimated at varying levels of approximation.

	$\bar{\chi}_{orb}^{PBE}$	$\bar{\chi}_{orb}^{B3LYP}$	$\bar{\chi}_{DFT*}^{PBE}$	$\bar{\chi}_{DFT*}^{B3LYP}$	$\bar{\chi}_{orb}^{HF}$	$\bar{\chi}^{MRCI}$	$\bar{\chi}_{IP}$
HF	144.294	148.368	165.107	165.458	163.001	165.352	157.156
H_2O	112.859	116.395	130.826	131.165	129.054	131.152	124.914
NH_3	85.841	88.942	101.305	101.666	99.909	101.658	95.572
CH_4	62.749	65.510	76.053	76.475	75.021	76.485	71.299
CO	123.005	126.875	142.145	142.587	140.662	142.451	135.047
N_2	120.140	124.040	139.036	139.541	137.882	139.391	132.114
CO_2	129.585	133.613	149.354	149.834	147.992	149.626	141.400
C_6H_6	85.49	88.78	101.47	101.91	100.46	[a]	94.30

[a] not computationally feasible.

Estimates to $\bar{\chi}$ obtained from the averaging of photoionization peaks, *i.e.*, $\bar{\chi}_{IP}$ values are in part provided as a small test set for the *experimental quantum chemistry* approach of Eq. (2). Estimates of $\bar{\chi}_{IP}$ are clearly smaller in absolute terms, compared to $\bar{\chi}_{DFT*}$, $\bar{\chi}_{orb}^{HF}$ and $\bar{\chi}^{MRCI}$, as expected from electronic relaxation effects.(*28*) We note however, that a linear regression of $\bar{\chi}^{MRCI}$and $\bar{\chi}_{IP}$ in these set of molecules have a coefficient of determination (r^2) of 0.9998, implying that relative measures, $\Delta\bar{\chi}$, can be productively approached experimentally.

Using $\bar{\chi}$ to Guide Density Functional Development

One way to use more physically motivated average electron energies, such as $\bar{\chi}_{DFT*}$ (ideally $\bar{\chi}_{DFT}$), is as a metric of quality of density functional approximations. DFT methods are today primarily evaluated against total energies and, to a lesser degree, properties.(*29*, *30*) The

average electron energy $\bar{\chi}$ contains twice all the terms most challenging in DFT functional design, those describing electron repulsion and correlation effects. All density functional approximations result in errors in both the density and in the computed XC energy for that density. Computations of total energies may therefore appear accurate because of fortuitous cancellations of these kinds of errors. By relying on $\bar{\chi}$ as a quality assessment, we offset such cancellations. Fig. 1 shows a selection of common functionals evaluated against the MRCI data of tables 1-3 (see also tables S4-S5). Our test set is not exhaustive and relies on the omission of T_c in the definition of $\bar{\chi}_{DFT*}$. Consequently, Fig. 1 data does not necessarily reflect the inherent quality of individual functionals. Instead, Fig. 1 is suggestive of an overall high quality of common DFT methods. Benchmarking of DFT methods using the formally exact $\bar{\chi}_{DFT}$ metric is outside of the scope of this work and has only been attempted for PBE.

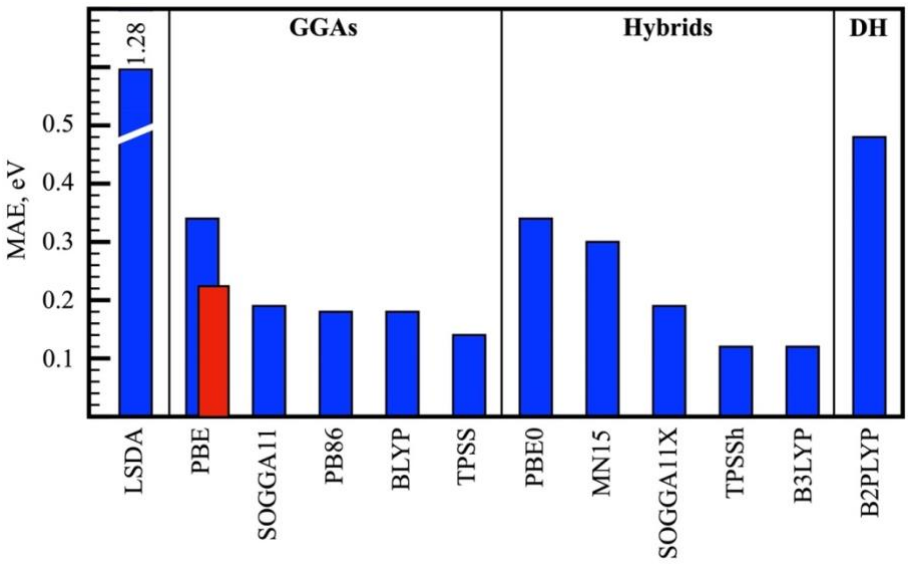

Figure 1: Mean-Average Error (MAE) of $\bar{\chi}_{DFT*}$ from $\bar{\chi}^{MRCI}$ computed with a selection of common density functional approximations. DH = double hybrid. The corresponding MAE for formally exact $\bar{\chi}_{DFT}$ is shown for PBE in red.

An on-the-fly Correction to KS Orbital Energies

Another way to utilize a more physically motivated average electron energy is for quantifying the impact of electron-electron interactions on KS orbitals. By using $\bar{\chi}_{DFT*}$ as a constraint on adjustments made to the fictitious one-particle KS energies we arrive at an interpretation of corrected levels that resembles the ionization-potential approximation to $\bar{\chi}$, Eq. (3). We have pointed out that the nature of $\bar{\chi}_{DFT}$ and $\bar{\chi}_{IP}$ differ. However, by adjusting the KS orbital energies subject to input from our formal-DFT analysis, we can make a new (and we think more physical) interpretation of the KS orbitals. We can view such adjusted levels as Fermi-golden-rule type representations as they would appear if independent-particle dynamics defined the average electron energy.

In what follows, we explore one correction scheme, in which the total energy of occupied orbitals is constrained so to equal the corrected total electron energy $N\bar{\chi}_{DFT*}$,

$$\sum_i n_i(\varepsilon_i + \Delta_i) = -N\bar{\chi}_{DFT*}, \tag{12}$$

where n_i is the occupation of orbital *i*, ε_i is the original orbital energy, and Δ_i is the amount by which orbital *i* is adjusted. The way by which Δ_i is determined is not necessarily unique. We here choose to correct each orbital by an amount that is directly proportional to its contribution to the total KS orbital average energy, $\bar{\chi}_{orb}^{KS}$, *i.e.*,

$$\Delta_i = \frac{\varepsilon_i}{\bar{\chi}_{orb}^{KS}}(\bar{\chi}_{orb}^{KS} - \bar{\chi}_{DFT*}). \tag{13}$$

The corrected energy of orbital *i*, ε_i^*, then becomes:

$$\varepsilon_i^* = \varepsilon_i \frac{\bar{\chi}_{DFT*}}{\bar{\chi}_{orb}^{KS}}. \tag{14}$$

In other words, the lower the energy of an occupied KS orbital the more it is corrected. The correction scheme of Eq. (14) appears to work well in general. Because we interpret the shifts as measures of the impact of exchange correlation on individual levels, we expect $\bar{\chi}$-constrained energies to lie *below* the (uncorrelated) HF references. Our results generally confirms that this observation holds despite using the simplest possible (linear) scheme for assigning level shifts. But we also note a caveat: The simple linear assignment may not be reliable to yield an accurate XC-content measure for 1s core levels. A more detailed analysis is necessary, but in the interest of simplicity we focus here on discussing the more chemically relevant valence orbitals. In practice, we proceed using pseudopotentials and ignore the 1s electrons altogether.

Fig. 2 shows an excerpt of our data where the correction scheme of Eq. (14) has been applied to standard DFT calculations performed on benzene (see also tables S6-S7). Additional examples are provided in tables S8-S9.

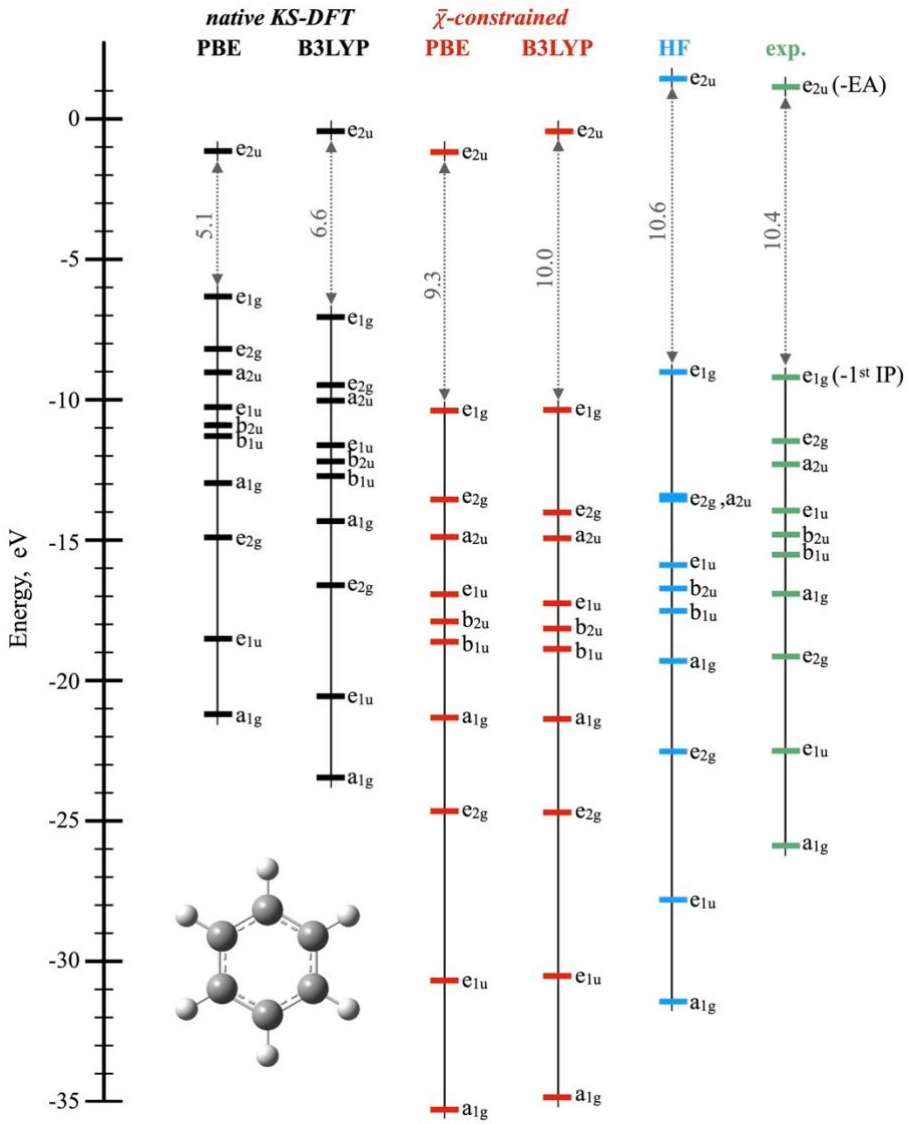

Figure 2: Native KS orbital eigenvalues (black), $\bar{\chi}$-constrained electron energies (red, adjusted following Eq. (14)) and Hartree-Fock orbital energies (blue) for benzene. Experimental data (green) from Ref. (*31*) are presented with negative signs to facilitate comparisons, and is subject to extensive relaxation effects during photoionization (*vide supra*). Occupied $\bar{\chi}$-constrained levels are largely independent on functional choice and describe electrons as more bound compared to Hartree-Fock. Energy gaps between occupied and unoccupied levels are indicated in grey. Symmetries (irreducible representations) of levels are indicated throughout.

Despite the simplicity of our correction scheme, an improvement is appreciable for all valence orbital energies when compared to experimental binding energies and especially to HF orbital energies. By *improvement* we refer to the general lowering of the energies attributed to each 1-particle wavefunction, an effect expected from a more physical accounting of electron correlation.

There are several consequences to our correction scheme: Unoccupied levels are unaffected, and the occupied higher levels, such as the HOMO, are only slightly corrected. That there should be a small correction for the HOMO orbital is in accord with Janack's theorem. Inner valence electrons are lowered by an increasing amount. A notable effect of our scheme is that the resulting energy levels are rather insensitive to the DFT functional (*c.f.* table S7). Increased agreement between levels of theory is particularly appreciable in molecules of many electrons. For example, the energy of the native KS HOMO of benzene differs by 0.62 eV when computed with PBE and B3LYP, while the $\bar{\chi}$-constrained HOMO level is predicted to be ~10.4 eV largely independent of the chosen XC approximation.

Conclusions

The usefulness of KS DFT derives from the construction of correlated electron densities from fictitious noninteracting electronic orbitals. One well known downside with this approach is that the resulting KS orbital energies have but tenuous connections to physical quantities. In this work we have derived an in principle exact expression for the average energy of *physical* electrons in DFT. Our inspiration for considering the average electron energy derives from chemistry, where this quantity has been linked to the useful concept of electronegativity.

A more physical description of electrons is demonstrated in several ways: The average electron energies of H, He^+ and H_2^+ computes as only fractions of an eV away from experimental ionization potentials using simple GGA functionals. Our approach provides a

more bound description of the average electron compared to HF theory in larger molecules and values consistently resemble those obtained at MRCI level of theory, but at drastically reduced computational costs. This agreement is a testament to how well self-interaction errors are handled in DFT. We therefore suggest that the average electron energy $\bar{\chi}$ can be used as a physically motivated (albeit non observable) indicator of quality, and as a constraint, in the design of DFT functionals.

A correction scheme for KS orbital energies is presented, which allows for a drastically better agreement with HF orbital eigenvalues and ionization potentials. This scheme is motivated as a physical constraint on otherwise fictitious KS energy levels, and as way to estimate the impact of electron-electron interactions on individual KS orbitals.

Our theory is straightforwardly implementable together with standard DFT functionals and software and comes at no additional computational cost. Implementation is here exemplified on molecular calculations, but applicability is being developed also for extended systems. Potential utility abounds: More physically motivated level energies will, for example, provide better predictions of chemical reactivity. Another tantalizing utility is the computation of more accurate band gaps. Such developments can lead to further improvements in the modeling of light-matter interactions, spectroscopy, electron transport and a range of material properties.

Acknowledgements

This work is dedicated to Neil Ashcroft who passed away on March 15, 2021.

Funding:

Chalmers University of Technology (MR)

The Carl Trygger Foundation grant 19:294 (MR)

The Swedish Foundation for Strategic Research contract IMF17-0324 (PH).

This research relied on computational resources provided by the Swedish National Infrastructure for Computing (SNIC) at C3SE, NSC and PDC partially funded by the Swedish Research Council through grant agreement no. 2018-05973.

Author contributions:

Conceptualization: MR

Investigation: SR, PH, PL, MR

Methodology: SR, PH, MR

Writing – original draft: MR, PH, SR

Competing interests: Authors declare that they have no competing interests.

Data and materials availability: All data are available in the main text or the supplementary materials. All used in-house code is available upon request.

Supplementary Materials

Materials and Methods

Supplementary Text

Reference and Notes *(31-62)*

Tables S1 to S9

References and Notes

1. J. P. Perdew, A. Zunger, Self-interaction correction to density-functional approximations for many-electron systems. *Phys. Rev. B.* **23**, 5048–5079 (1981).
2. A. J. Cohen, P. Mori-Sánchez, W. Yang, Insights into Current Limitations of Density Functional Theory. *Science (80-.).* **321**, 792–794 (2008).
3. T. Schmidt, E. Kraisler, L. Kronik, S. Kümmel, One-electron self-interaction and the asymptotics of the Kohn-Sham potential: An impaired relation. *Phys. Chem. Chem.*

Phys. **16**, 14357–14367 (2014).

4. P. Sjoberg, J. S. Murray, T. Brinck, P. Politzer, Average local ionization energies on the molecular surfaces of aromatic systems as guides to chemical reactivity. *Can. J. Chem.* **68**, 1440–1443 (1990).
5. P. Politzer, J. S. Murray, F. A. Bulat, Average local ionization energy: A review. *J. Mol. Model.* **16**, 1731–1742 (2010).
6. D. G. Pettifor, *Bonding and Structure of Molecules and Solids* (Oxford University Press, New York, 1995).
7. L. C. Allen, Electronegativity Is the Average One-Electron Energy of the Valence-Shell Electrons in Ground-State Free Atoms. *J. Am. Chem. Soc.* **111**, 9003–9014 (1989).
8. M. Rahm, R. Hoffmann, Distinguishing Bonds. *J. Am. Chem. Soc.* **138**, 3731–3744 (2016).
9. M. Rahm, R. Hoffmann, Toward an experimental quantum chemistry: Exploring a new energy partitioning. *J. Am. Chem. Soc.* **137**, 10282–10291 (2015).
10. M. Rahm, T. Zeng, R. Hoffmann, Electronegativity Seen as the Ground State Average Valence Electron Binding Energy. *J. Am. Chem. Soc.* **141**, 342–351 (2019).
11. S. Racioppi, M. Rahm, In Situ Electronegativity and the Bridging of Chemical Bonding Concepts. *Chem. – A Eur. J.* (2021), doi:10.1002/chem.202103477.
12. M. Rahm, R. Cammi, N. W. Ashcroft, R. Hoffmann, Squeezing All Elements in the Periodic Table: Electron Configuration and Electronegativity of the Atoms under Compression. *J. Am. Chem. Soc.* **141**, 10253–10271 (2019).
13. T. Koopmans, The classification of wave functions and eigen-values to the single electrons of an atom. *Physica*. **1**, 104–113 (1934).
14. O. V. Gritsenko, B. Braïda, E. J. Baerends, Physical interpretation and evaluation of

the Kohn-Sham and Dyson components of the ε-I relations between the Kohn-Sham orbital energies and the ionization potentials. *J. Chem. Phys.* **119**, 1937–1950 (2003).

15. P. Hyldgaard, Y. Jiao, V. Shukla, Screening nature of the van der Waals density functional method: A review and analysis of the many-body physics foundation. *J. Phys. Condens. Matter*. **32**, 393001 (2020).
16. J. F. Janak, Proof that dE/dni=ei in density-functional theory. *Phys. Rev. B.* **18**, 7165–7168 (1978).
17. E. Kraisler, L. Kronik, Piecewise linearity of approximate density functionals revisited: Implications for frontier orbital energies. *Phys. Rev. Lett.* **110**, 1–5 (2013).
18. W. Kohn, L. J. Sham, Self-Consistent Equations Including Exchange and Correlation Effects. *Phys. Rev. Rev.* **140**, A1133–A1138 (1965).
19. M. Levy, J. P. Perdew, Hellman-Feynman, virial, and scaling properties for the exact universal denisty function. Shape of the correlation potential and diamagnetic susceptibility for atoms. *Phys. Rev. A.* **32**, 2010–2021 (1985).
20. M. Mundt, S. Kümmel, B. Huber, M. Moseler, Photoelectron spectra of sodium clusters: The problem of interpreting Kohn-Sham eigenvalues. *Phys. Rev. B - Condens. Matter Mater. Phys.* **73**, 1–6 (2006).
21. Y. Jiao, E. Schröder, P. Hyldgaard, *Phys. Rev. B* **97**, 085115 1-15 (2018).
22. J. K. Burdett, S. Lee, Moments and the Energies of Solids. *J. Am. Chem. Soc.* **107**, 3050–3063 (1985).
23. J. P. Perdew, K. Burke, M. Ernzerhof, D. of Physics, N. O. L. 70118 J. Quantum Theory Group Tulane University, Generalized Gradient Approximation Made Simple. *Phys. Rev. Lett.* **77**, 3865–3868 (1996).
24. A. D. Becke, Density-functional thermochemistry.III. The role of exact exchange. *J. Chem. Phys.* **98**, 5648 (1993).

25. C. Lee, W. Yang, R. G. Parr, Development of the Colle-Salvetti correlation-energy formula into a functional of the electron density. *Phys. Rev. B.* **37**, 785–789 (1988).

26. P. S. Bagus, E. S. Ilton, C. J. Nelin, The interpretation of XPS spectra: Insights into materials properties. *Surf. Sci. Rep.* **68**, 273–304 (2013).

27. P. S. Bagus, Self-consistent-field wave functions for hole states of some Ne-like and Ar-Like ions. *Phys. Rev.* **139**, 619–634 (1965).

28. L. S. Cederbaum, W. Domcke, J. Schirmer, W. Von Niessen, Correlation Effects in the Ionization of Molecules: Breakdown of the Molecular Orbital Picture. *Adv. Phys.* **65**, 115–159 (1986).

29. A. Patra, J. E. Bates, J. Sun, J. P. Perdew, Properties of real metallic surfaces: Effects of density functional semilocality and van der Waals nonlocality. *Proc. Natl. Acad. Sci. U. S. A.* **114**, E9188–E9196 (2017).

30. M. G. Medvedev, I. S. Bushmarinov, J. Sun, J. P. Perdew, K. A. Lyssenko, Density functional theory is straying from the path toward the exact functional. *Science (80-.).* **356**, 496c (2017).

31. T. A. Carlson, P. Gerard, M. O. Krause, F. A. Grimm, B. P. Pullen, Photoelectron dynamics of the valence shells of benzene as a function of photon energy. *J. Chem. Phys.* **86**, 6918–6926 (1987).

32. R. B. 0. Gaussian 16, M. J. Frisch, G. W. Trucks, H. B. Schlegel, G. E. Scuseria, M. A. Robb, J. R. Cheeseman, G. Scalmani, V. Barone, G. A. Petersson, H. Nakatsuji, X. Li, M. Caricato, A. V. Marenich, J. Bloino, B. G. Janesko, R. Gomperts, B. Mennucci, H. P. Hratchian, J. V. Ortiz, A. F. Izmaylov, J. L. Sonnenberg, D. Williams-Young, F. Ding, F. Lipparini, F. Egidi, J. Goings, B. Peng, A. Petrone, T. Henderson, D. Ranasinghe, V. G. Zakrzewski, J. Gao, N. Rega, G. Zheng, W. Liang, M. Hada, M. Ehara, K. Toyota, R. Fukuda, J. Hasegawa, M. Ishida, T. Nakajima, Y. Honda, O.

Kitao, H. Nakai, T. Vreven, K. Throssell, J. A. M. Jr., J. E. Peralta, F. Ogliaro, M. J. Bearpark, J. J. Heyd, E. N. Brothers, K. N. Kudin, V. N. Staroverov, T. A. Keith, R. Kobayashi, J. Normand, K. Raghavachari, A. P. Rendell, J. C. Burant, S. S. Iyengar, J. Tomasi, M. Cossi, J. M. Millam, M. Klene, C. Adamo, R. Cammi, J. W. Ochterski, R. L. Martin, K. Morokuma, O. Farkas, J. B. Foresman, D. J. Fox, Gaussian16 (2016), p. Gaussian, Inc., Wallingford CT.

33. W. J. Stevens, H. Basch, M. Krauss, Compact effective potentials and efficient shared-exponent basis sets for the first- and second-row atoms. *J. Chem. Phys.* **81**, 6026–6033 (1984).

34. H. J. Werner, P. J. Knowles, G. Knizia, F. R. Manby, M. Schütz, Molpro: A general-purpose quantum chemistry program package. *Wiley Interdiscip. Rev. Comput. Mol. Sci.* **2**, 242–253 (2012).

35. P. G. Szalay, T. Müller, G. Gidofalvi, H. Lischka, R. Shepard, Multiconfiguration self-consistent field and multireference configuration interaction methods and applications. *Chem. Rev.* **112**, 108–181 (2012).

36. H. J. Werner, P. J. Knowles, A second order multiconfiguration SCF procedure with optimum convergence. *J. Chem. Phys.* **82**, 5053–5063 (1985).

37. D. E. Woon, T. H. Dunning, Gaussian basis sets for use in correlated molecular calculations. V. Core-valence basis sets for boron through neon. *J. Chem. Phys.* **103**, 4572–4585 (1995).

38. M. S. Banna, D. A. Shirley, Molecular photoelectron spectroscopy at 123.3 eV. The second-row hydrides. *J. Phys. Chem.* **63**, 4759–4766 (1975).

39. D. A. Allison, R. G. Cavell, Photoelectron spectroscopy with Zr Mζ(151 eV) radiation. A study of the variation of relative photoionization cross sections of molecules containing first row atoms (C, N, O) with exciting radiation from HeIto Mg Kαlimits.

J. Chem. Phys. **68**, 593–601 (1978).

40. K. Siegbahn, C. Nordling, G. Johansson, J. Hedman, P. F. Hedén, K. Hamrin, U. Gelius, T. Bergmark, L. O. Werme, R. Manne, *ESCA Applied to Free Molecules* (North Holland Publ. Co., Amsterdam - London, 1969).

41. C. J. Allan, K. Siegbahn, U. Gelius, D. A. Allison, G. Johansson, H. Siegbahn, ESCA studies of CO2, CS2 and COS. *J. Electron Spectros. Relat. Phenomena*. **1**, 131–151 (1972).

42. P. Giannozzi, S. Baroni, N. Bonini, M. Calandra, R. Car, C. Cavazzoni, D. Ceresoli, G. L. Chiarotti, M. Cococcioni, I. Dabo, A. Dal Corso, S. De Gironcoli, S. Fabris, G. Fratesi, R. Gebauer, U. Gerstmann, C. Gougoussis, A. Kokalj, M. Lazzeri, L. Martin-Samos, N. Marzari, F. Mauri, R. Mazzarello, S. Paolini, A. Pasquarello, L. Paulatto, C. Sbraccia, S. Scandolo, G. Sclauzero, A. P. Seitsonen, A. Smogunov, P. Umari, R. M. Wentzcovitch, QUANTUM ESPRESSO: A modular and open-source software project for quantum simulations of materials. *J. Phys. Condens. Matter*. **21** (2009), doi:10.1088/0953-8984/21/39/395502.

43. D. R. Hamann, Optimized norm-conserving Vanderbilt pseudopotentials. *Phys. Rev. B - Condens. Matter Mater. Phys.* **88**, 1–10 (2013).

44. N. D. Mermin, Thermal properties of the inhomogeneous electron gas. *Phys. Rev.* **137**, 1–3 (1965).

45. O. V. Gritsenko, R. Van Leeuwen, E. J. Baerends, Molecular exchange-correlation Kohn-Sham potential and energy density from ab initio first- and second-order density matrices: Examples for XH (X=Li, B, F). *J. Chem. Phys.* **104**, 8535–8545 (1996).

46. V. N. Staroverov, G. E. Scuseria, J. Tao, J. P. Perdew, Comparative assessment of a new nonempirical density functional: Molecules and hydrogen-bonded complexes. *J. Chem. Phys.* **119**, 12129–12137 (2003).

47. X. Xu, W. A. Goddard, The X3LYP extended density functional for accurate descriptions of nonbond interactions, spin states, and thermochemical properties. *Proc. Natl. Acad. Sci. U. S. A.* **101**, 2673–2677 (2004).

48. J. Tao, J. P. Perdew, V. N. Staroverov, G. E. Scuseria, Climbing the density functional ladder: Nonempirical meta–generalized gradient approximation designed for molecules and solids. *Phys. Rev. Lett.* **91**, 3–6 (2003).

49. A. J. Cohen, N. C. Handy, Dynamic correlation. *Mol. Phys.* **99**, 607–615 (2001).

50. C. Adamo, V. Barone, Toward reliable adiabatic connection models free from adjustable parameters. *Chem. Phys. Lett.* **274**, 242–250 (1997).

51. A. D. Becke, Density-functional exchange-energy approximation with correct asymptotic behavior. *Phys. Rev. A.* **38**, 3098–3100 (1988).

52. J. P. Perdew, Density-functional approximation for the correlation energy of the inhomogeneous electron gas. *Phys. Rev. B.* **33**, 8822–8824 (1986).

53. D. J. Lacks, R. G. Gordon, Pair interactions of rare-gas atoms as a test of exchange-energy-density functionals in regions of large density gradients. *Phys. Rev. A.* **47**, 4681–4690 (1993).

54. R. Peverati, Y. Zhao, D. G. Truhlar, Generalized gradient approximation that recovers the second-order density-gradient expansion with optimized across-the-board performance. *J. Phys. Chem. Lett.* **2**, 1991–1997 (2011).

55. R. Peverati, D. G. Truhlar, Communication: A global hybrid generalized gradient approximation to the exchange-correlation functional that satisfies the second-order density-gradient constraint and has broad applicability in chemistry. *J. Chem. Phys.* **135** (2011), doi:10.1063/1.3663871.

56. H. S. Yu, X. He, S. L. Li, D. G. Truhlar, MN15: A Kohn–Sham global-hybrid exchange–correlation density functional with broad accuracy for multi-reference and

single-reference systems and noncovalent interactions. *Chem. Sci.* **7**, 5032–5051 (2016).

57. Y. Zhao, D. G. Truhlar, Design of density functionals that are broadly accurate for thermochemistry, thermochemical kinetics, and nonbonded interactions. *J. Phys. Chem. A.* **109**, 5656–5667 (2005).

58. C. Adamo, V. Barone, Toward reliable density functional methods without adjustable parameters: The PBE0 model. *J. Chem. Phys.* **110**, 6158–6170 (1999).

59. R. Peverati, D. G. Truhlar, M11-L: A local density functional that provides improved accuracy for electronic structure calculations in chemistry and physics. *J. Phys. Chem. Lett.* **3**, 117–124 (2012).

60. S. Grimme, Semiempirical hybrid density functional with perturbative second-order correlation. *J. Chem. Phys.* **124** (2006), doi:10.1063/1.2148954.

61. J. C. Slater, *Quantum Theory of Molecular and Solids. The Self-Consistent Field for Molecular and Solids* (McGraw-Hill, New York, 1974), vol. 4.

62. S. H. Vosko, L. Wilk, M. Nusair, Accurate spin-dependent electron liquid correlation energies for local spin density calculations: a critical analysis. *Can. J. Phys.* **58**, 1200–1211 (1980).